View metadata, citation and similar papers at core.ac.uk

brought to you by CORE

doi:10.14311/ppt.2017.1.28
Plasma Physics and Technology **4**(1):28–31, 2017
© Department of Physics, FEE CTU in Prague, 2017

PLASMA ASSISTED GENERATION OF MICRO- AND NANOPARTICLES

A. Veklich[a,*], A. Lebid[a], T. Tmenova[a], V. Boretskij[a], Y. Cressault[b], F. Valensi[b], K. Lopatko[c], Y. Aftandilyants[c]

[a] *Taras Shevchenko National University of Kyiv, 64/13, Volodymyrska str., Kyiv, Ukraine*

[b] *Université de Toulouse; UPS, INPT; LAPLACE (Laboratoire Plasma et Conversion d'Energie); 118 route de Narbonne, F-31062 Toulouse Cedex 9, France*

[c] *National University of Life and Environmental Sciences of Ukraine, Kiev, Ukraine*

[*] van@univ.kiev.ua

Abstract. In this research, the peculiarities of micro- and nanoparticles generation are considered. Two techniques of micro- and nanoparticles' formation using electric arc and underwater discharge plasma sources are proposed. Molybdenum oxide crystals were deposited on side surface of the bottom electrode (anode) of the free-burning discharge between metallic molybdenum electrodes. Friable layer of MoO_3, which consists of variously oriented transparent prisms and platelets (up to few hundreds of μm in size), was formed by vapor deposition around the electrode. In the second technique, plasma of the underwater electric spark discharges between metal granules was used to obtain stable colloidal solutions with nanoparticles of 20–100 nm sizes.

Keywords: molybdenum trioxide, plasma evaporation, underwater spark discharge, colloidal liquids.

1. Introduction

Plasma treatment of materials attracts strong interest due to extreme conditions of processes, which can't be achieved in other way. Particularly, plasma technology can be used for fabrication of materials structured on micro- and nanoscale [1, 2]. Application of such materials can significantly improve existing industrial and biological technologies. For example, molybdenum trioxide crystals can be used in solar cells [3], lithium-ion batteries [4, 5], chemical catalysis [6] and gaseous sensors [7]. At the same time, solutions of metallic nanoparticles are already being used for purposes of biological and food applications [8, 9]. Fundamental difference between the colloidal and conventional forms of mineral nutrients is that the first are non-toxic, bioavailable and by virtue of the crystalline structure of the dispersed phase are the most suitable for their use on biological objects. Such metal colloids exhibit high efficacy and have already found their application in the cultivation of vegetable production under conditions of low or disturbed mineral nutrition [8, 9]. Nowadays, plasma assisted technologies are very effective for micro- and nanomaterials generation. Cheapness of such technologies has made them attractive for solution of different scientific and applied problems.

This work deals with two alternative plasma assisted techniques of micro- and nanoparticles generation. Technique of micro structured molybdenum trioxide crystal fabrication in electric arc plasma source and alternative technique of metal nanoparticles generation in underwater spark discharge is described. Main processes stages and material properties are discussed.

2. Techniques of micro- and nanoparticles generation

2.1. Micro-structured molybdenum trioxide crystal fabrication in electric arc plasma source

The vertically oriented free-burning arc was ignited in air between the end surfaces of metallic molybdenum non-cooled electrodes (See Fig.1). The diameter of the rod electrodes was 6 mm, the discharge gap was 8 mm and DC current was 3.5 A. Molybdenum oxide crystals were deposited on the side surface of anode [10]. It must be noted, that the formation of crystals takes place 3-5 mm below the end surface of electrode.

2.2. Underwater spark discharge for production of nanoparticles solution

Colloidal solutions of metal particles are obtained by realization of volumetric electric spark destruction of metal granules. This method lies in the simultaneous formation of spark channels in contacts between metal granules immersed in a liquid. Electric energy was supplied by specially developed pulse generator [11]. As a result of spark erosion, part of metal granules evaporates and, while being tempered into a liquid, forms fine dispersion fraction of spark-erosive particles. The plasma of underwater electric spark discharges between metal granules was used to obtain stable colloidal solutions with nanoparticles of 20-100 nm sizes. The experimental values of voltage were up to 300 V, current - up to 600 A and the capacity of the discharge circuit - up to 1300 μF.

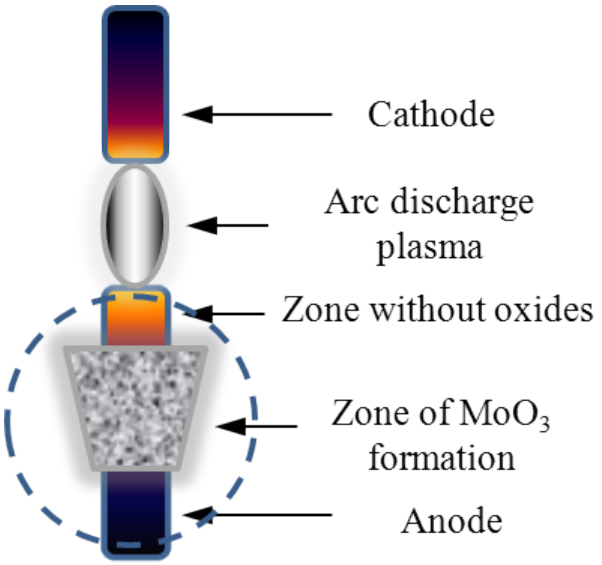

Figure 1. Electrodes arrangement for fabrication of MoO_3 crystals

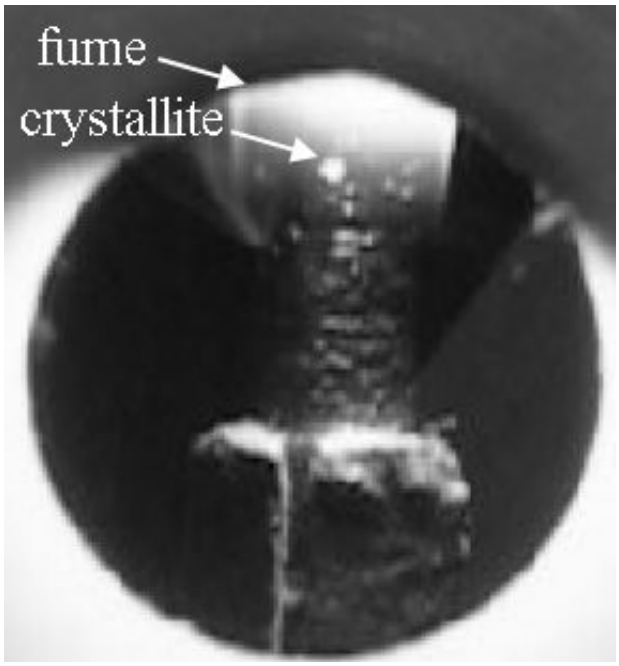

Figure 2. Formation of MoO_3 crystallites.

3. Results and discussions

3.1. Micro-structured MoO_3

The process of crystals formation during arc discharge can be divided into specific sequential stages. Immediately after arc ignition there was no evaporation due to relatively low initial temperature of the anode surface.

Few seconds after, a white fume was observed around the electrode (See Fig.2). This stage can be explained by oxidation of metallic molybdenum and volatilization of oxides as the electrode temperature increases. The oxidation of metallic molybdenum surface and volatilization of the oxide layer were observed during heating in the furnace. The MoO_3 crystallites appeared on the electrode surface during the next process phase (See Fig.2). Crystals start growing from white fume evaporations, which are transported by convectional air flow. Probably, initial crystallization starts on surface defects or on greyish-black particles. Friable layer around electrode, which consists of variously oriented transparent prisms and platelets, was formed by vapor deposition.

It was mentioned in [12] that oxide layer completely evaporates from molybdenum surface at temperature above 1150° C. Therefore, this assumption explains the absence of crystals near the end surface of electrode wherein surface temperature is obviously higher.

Re-evaporation of deposited crystals is absent because of two reasons. The first one is low thermal conductivity between electrode and crystallites due to their irregular orientation. The crystallites are weakly connected to the electrode surface but have numerous connections with each other. The second reason is cooling of crystallites by convectional flows.

Chemical composition and structure of produced crystals were determined by X-rays diffraction method (XRD). Obtained crystals were detached from electrode surface and milled before the investigations. X-ray diffraction study indicates that resulting crystals consist of orthorhombic α-MoO_3 phase. Only small amount of monoclinic β-MoO_3 phase was detected.

Optical microscopy studies indicate formation of feather-like structures (Fig.3). Every "feather" consists of closely packed parallel needles, which are unfinished structures of directional crystal growth. These needles are resembled to microrods observed in [4], but in contrast, these microrods have random orientation. Probably, attachment of building material on these pins takes place during the vapor deposition process and supports further translation of crystal structure.

3.2. Peculiarities of metal nanoparticles generation

The study of energy dissipation channels in underwater discharges can clarify the most effective mechanisms of nanoparticles' generation. Therefore, it is essential to determine the excitation temperature of metal atoms in discharge plasma.

Optical emission spectroscopy (OES) methods were used for diagnostics of the underwater electric spark discharge plasma between metal granules. Plasma emission was registered by the SDH-IV spectrometer with a 4-position manually switchable diffraction gratings turret. The measurements were performed in all four channels of spectrometer, so the total registered spectral range was 200-1200 nm. Toshiba TCD 1304 AP linear image sensor was used as CCD detector. Spectral sensitivity in every spectral range of the SDH-IV spectrometer was determined and taken into account.

Experiments with granules of Cu, Fe, Mn and Mo were performed. Emission spectra of corresponding

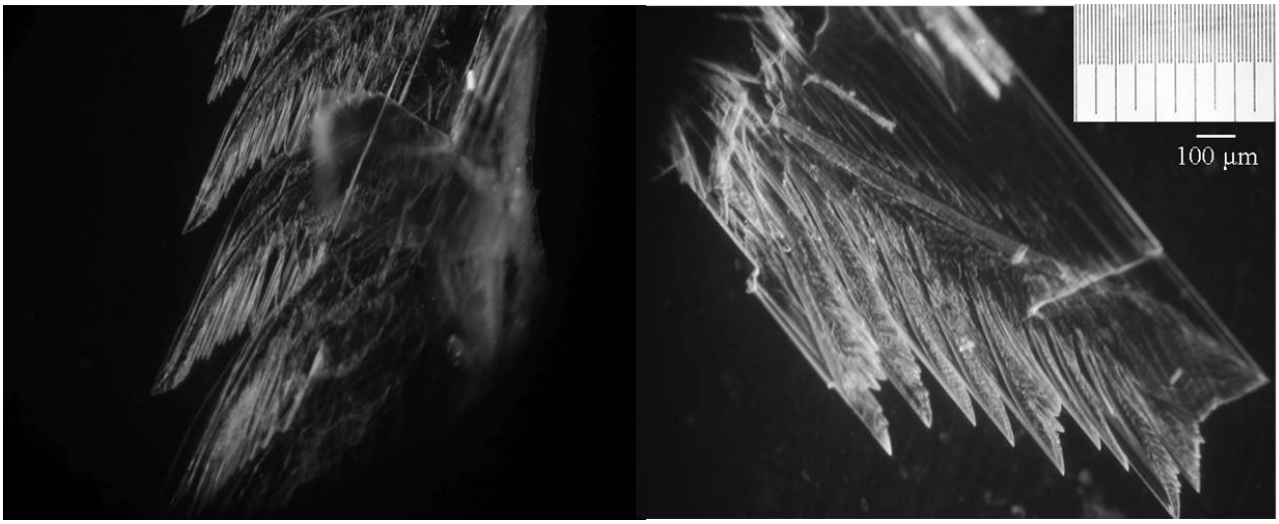

Figure 3. Images of α-MoO_3 crystallite from different view angles

elements were obtained using OES techniques. As an example, the emission spectrum of the discharge between manganese granules is shown in Fig.4 together with the relative emission of manganese lines from NIST database [13]. One can see that the spectrum contains mainly metal emissions lines (Mn I and Mn II). For discharges between copper granules [11] we also observed oxygen triplet (λ=777 nm), and hydrogen Balmer H_α and H_β lines, which are typical for emission spectrum of the electric discharge plasma in water [14].

The excitation temperature of manganese ions in plasma was determined by Boltzmann plot technique using Mn II spectral lines 345.94, 347.32, 349.55, 432.61, 434.37 and 530.11 nm under assumption of Boltzmann distribution of population of ion's energy levels. Spectroscopic data for these lines were used from [13]. Fig.5 shows the Boltzmann plot for emission of Mn II lines derived from spectrum presented in Fig.4. The slope of the line in this Boltzmann plot gives the value of the excitation temperature of 9000 K. Similar estimation of the excitation temperature in discharge between copper granules showed the values of 12000±2000 K [11]. Spectral lines of Cu I 456.1, 510.5, 515.3, 521.8, 570.0, 578.2, 793.3 and 809.2 nm were used in this case. Spectroscopic data for these lines were used from [15].

4. Conclusions

Self-organized vapor-deposition process of MoO_3 crystals formation takes place in the proposed plasma source. The investigation of crystal formation zone allows to confirm the following process mechanisms: molybdenum surface oxidation, evaporation of oxide layer, vapour transportation by convectional air flow and crystal growth.

Studies of plasma of the underwater electric spark discharge with granules of Cu, Fe, Mn and Mo were carried out. Detailed investigation of such discharge plasma between manganese and copper granules was performed. The emission spectra of plasma and its excitation temperature were obtained using OES techniques. The obtained results show that values of the excitation temperatures of 12000 K and 9000 K were obtained in underwater discharge plasma between copper and manganese, respectively.

References

[1] P. Badica. Preparation through the vapor transport and growth mechanism of the first-order hierarchical structures of MoO_3 belts on siliminite fiber. *Crystal growth and design*, 7(4):794–801, 2007. doi:10.1021/cg060893s.

[2] A Laviña, J.A. Aznárez, and C. Ortiz. Electron microscopy study of some molybdenum oxide crystals. *Journal of Crystal Growth*, 48:100–106, 1980. doi:10.1016/0022-0248(80)90198-0.

[3] D. Mariotti, T. Belmonte, J. Benedikt, T. Velusamy, G. Jain, and V. Švrček. Low-temperature atmospheric pressure plasma processes for "green" third generation photovoltaics. *Plasma Processes and Polymers*, 13:70–90, 2016. doi:10.1002/ppap.201500187.

[4] W. Li, F. Cheng, Z. Tao, and J. Chen. Vapor-transportation preparation and reversible lithium intercalation/deintercalation of α-MoO_3 microrods. *J. Phys. Chem. B*, 110:119–124, 2006. doi:10.1021/jp0553784.

[5] D. Mariotti, H. Lindstrom, A. Chandra Bose, and K. Ostrikov. Monoclinic α-MoO_3 nanosheets produced by atmospheric microplasma: application to lithium-ion batteries. *Nanotechnology*, 19:49530, 2008. doi:10.1088/0957-4484/19/49/495302.

[6] K. T. Queeney and C. M. Friend. Site-selective surface reactions: hydrocarbon oxidation processes on oxidized Mo(110). *J. Phys. Chem. B*, 104:409–415, 2000. doi:0.1021/jp991994m.

[7] E Comini, G Faglia, G Sberveglieri, C Cantlini, M Passacantando, S Santucci, Y Li, W Wlodarski, and W Qu. Carbon monoxide response of molybdenum oxide thin films deposited by different techniques.

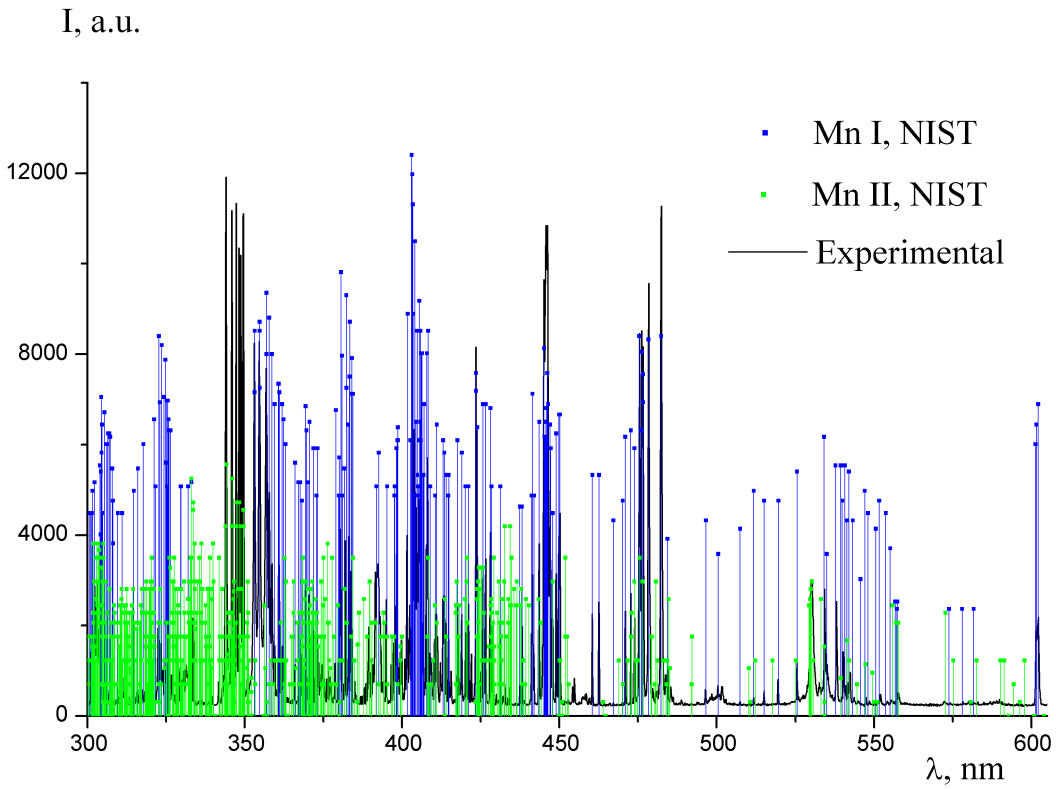

Figure 4. Emission spectrum of plasma of underwater electric spark discharge between granules of Mn.

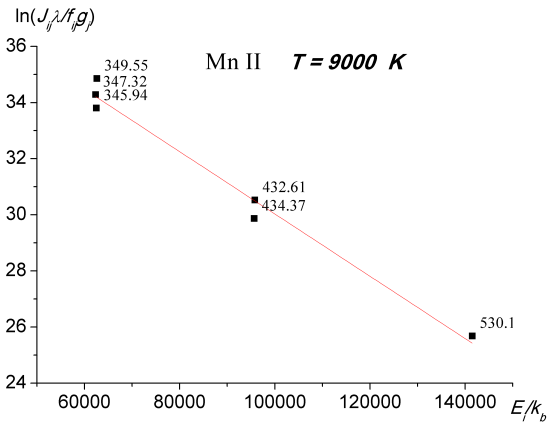

Figure 5. Boltzmann plot for calculation of excitation temperature of the underwater spark discharge plasma between Mn granules.

Sensors and Actuators B, 68:168–174, 2008. doi:10.1016/S0925-4005(00)00484-6.

[8] N. Taran, O. Gonchar, and Lopatko K. The effect of colloidal solution of molybdenum nanoparticles on the microbial composition in rhizosphere of cicer arietinum l. *Nanoscale Res Lett.*, 9:289, 2014. doi:10.1186/1556-276X-9-289.

[9] D. Ehrhardt and W. Frommer. New technologies for 21st century plant science. *The Plant Cell*, 24(2):374–394, 2012. doi:10.1105/tpc.111.093302.

[10] A. Lebid, V. Boretskij, S. Savenok, A. Veklich, and O. Andreev. Thermal plasma source for processing of MoO_3 crystals. *J. Phys.: Conf. Ser.*, 550:012027, 2014. doi:10.1088/1742-6596/550/1/012027.

[11] T. Tmenova, A. Veklich, V. Boretskij, Y. Cressault, F. Valensi, K. Lopatko, and Y. Aftandilyants. Optical emission spectroscopy of plasma of underwater electric spark discharges between metal granules. *Problems of Atomic Science and Technology. Series: Plasma Physics*, 107(23):132–135, 2017.

[12] Vahldiek F.W. Growth and microstructure of molybdenum oxide. *Journal of the Less-Common Metals*, 16:351–359, 1968. doi:10.1016/0022-5088(68)90132-X.

[13] A. Kramida, Yu. Ralchenko, J. Reader, and and NIST ASD Team. NIST Atomic Spectra Database (ver. 5.3), [Online]. Available: http://physics.nist.gov/asd [2017, May 1]. National Institute of Standards and Technology, Gaithersburg, MD., 2015.

[14] H. Li, J. Kang, and K. Urashima. Comparison between the mechanism of liquid plasma discharge process in water and organic solution. *J. Inst. Electrostat. Jpn.*, 37(1):22–27, 2013.

[15] I. Babich, V. Boretskij, A. Veklich, and R. Semenyshyn. Spectroscopic data and stark broadening of cu i and ag i spectral lines: Selection and analysis. *Advances in Space Research*, 54:1254–1263, 2014. doi:10.1016/j.asr.2013.10.034.